

PACS numbers: 42.81.Wg; 42.40.Eq
DOI: 10.1070/QE2012v042n09ABEH014962

Suppression of side lobes in a spectrum of fibre Bragg gratings due to the transverse displacement of phase mask with respect to the optical fibre

S.R. Abdullina, I.N. Nemov, S.A. Babin

Abstract. **The possibility of apodisation of fibre Bragg gratings (FBGs) recorded in the interference region of two Gaussian beams in the phase-mask scheme is considered. The FBG reflection spectra are numerically simulated for different values of recording-beam parameters and the distance between the axes of interfering beams diffracted into different orders, which is varied by transverse displacement of the phase mask with respect to the optical fibre. Suppression of side lobes and smoothing out of the FBG spectrum with an increase in the transverse displacement of the phase mask is experimentally demonstrated. It is shown that this effect is caused by the equalisation of the mean induced refractive index in the FBG region.**

Keywords: *fibre Bragg grating, apodisation, reflection spectrum.*

1. Introduction

Currently fibre Bragg gratings (FBGs) are widely used in various fibre optics devices, in particular, as fibre laser mirrors, sensors, and elements of multiplexers and demultiplexers. Specific applications impose certain requirements on the shape of FBG spectrum, which is determined by the profile of the grating refractive index. One of the most general requirements is the absence of side lobes, which is obtained by the so-called apodisation: a smooth change in the modulation amplitude and equalisation of the mean induced refractive index along the grating [1–4].

A phase mask is often used to form an interference pattern when a grating is recorded by UV radiation. In this case, apodisation is performed by longitudinal scanning of a focused laser beam with respect to the optical fibre and mask [5, 6]. During scanning one can modulate the relative position of the optical fibre and the phase mask using piezoelectric ceramic, as a result of which the interference pattern becomes blurred. Changing the modulation amplitude step by step, one can form a specified grating profile at a constant mean refractive index, which makes it possible to suppress the lateral-resonance amplitude in the FBG spectrum to –35 dB [1, 5]. This way is universal (with respect to the form of apodising function) but is rather difficult to implement.

A simpler technique for suppressing side lobes in FBG spectra (without scanning the beam with respect to the optical fibre and mask) was proposed in [7]. In the first stage an optical fibre is exposed to a stationary interference pattern, whose profile is set by the Gaussian intensity profile of the interfering beams formed by a phase mask. In the second stage, the mean induced refractive index is equalised by postexposure of the optical fibre to one Gaussian beam at a distance of the order of its radius, on the left and on the right from the centre of the FBG recorded. Being relatively simple, this way, nevertheless, turned out to be rather efficient: the side lobes for gratings with a reflection coefficient $R \sim 0.98$ were suppressed to a level below –20 dB, which is determined by the spectrometer sensitivity.

In this study, we consider another possibility of equalising the mean induced refractive index in the phase-mask scheme, which is based on relative displacement of the centres of interfering Gaussian beams. When a phase mask is used, it is generally assumed that the fibre is located directly behind the mask and that the axes of interfering beams of the +1st and –1st diffraction orders practically coincide. However, when the mask is displaced by some distance δl in the transverse direction with respect to the fibre (Fig. 1), an FBG is recorded in the interference region of two Gaussian beams, the axes of which diverge at a distance $2\delta z$, where $\delta z = \delta l \tan\alpha$ and α is the half angle between the directions of the +1st and –1st diffraction orders (in our case $\alpha = 13.5°$). The $z = 0$ axis is the bisector of the angle made by the axes of interfering beams.

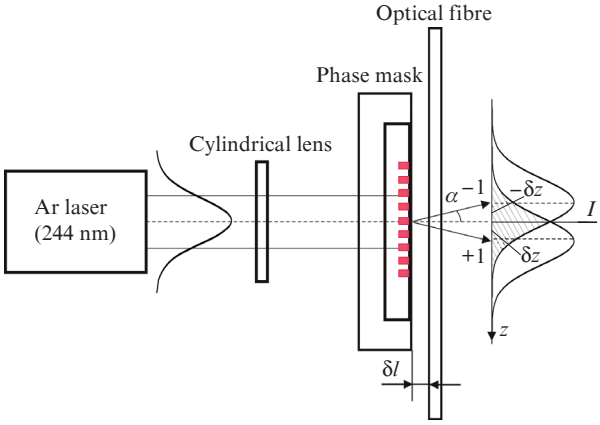

Figure 1. Scheme of FBG recording. On the right: the intensity distributions for the beams diffracted into the +1st and –1st orders in the optical fibre core in the presence of relative displacement $\delta z = \delta l \tan\alpha$, which is determined by the displacement δl of the phase mask with respect to the optical fibre. The interference region is hatched.

S.R. Abdullina, I.N. Nemov, S.A. Babin Institute of Automation and Electrometry, Siberian Branch, Russian Academy of Sciences, ul. Akad. Koptyuga 1, 630090 Novosibirsk, Russia; e-mail: sonka@ngs.ru

Received 27 July 2012
Kvantovaya Elektronika **42** (9) 794–798 (2012)
Translated by Yu.P. Sin'kov

To analyse the effect, we calculated the FBG spectra at different displacements δl of the phase mask with respect to the optical fibre and performed test experiments. The calculation results and experimental data are reported below.

2. Calculation

The FBG spectra were numerically simulated by the technique described in detail in [7], using the programs supplied by Belai et al. [8]. Prior to recording, the fibre refractive index n_0 was 1.468.

An FBG is recorded in the interference region of the beams diffracted into the +1st and –1st orders of the phase mask. The profile of phase-mask lines provides suppression of zero-order diffraction to 7% and concentration of 75% recording beam power in the +1st and –1st orders. On the assumption that the change in the refractive index depends linearly on intensity, the profile of the induced refractive index in the interference region of the beams with axes shifted by δz (see Fig. 1) has the form

$$\Delta n(z) = \delta m \Delta n_0 \left[\exp\left(-\frac{2(z-\delta z)^2}{w^2}\right) + \exp\left(-\frac{2(z+\delta z)^2}{w^2}\right)\right] \times \left[1 + \frac{f(z,\delta z)}{\cosh(4z\delta z/w^2)}\cos\left(\frac{2\pi}{\Lambda}z\right)\right] + \delta m_0 \Delta n_0 \exp\left(-\frac{2z^2}{w^2}\right). \quad (1)$$

Here, w is the radius of the Gaussian beam incident on the mask; Δn_0 is the amplitude of change in the induced refractive index in the intensity maximum; $\delta m = 0.375$ are the power fractions in the +1st and –1st orders; $\delta m_0 = 0.07$ is the zero-order power fraction; z is the coordinate along the grating; Λ is the interference pattern period; and $f(z, \delta z)$ is the coherence function [$f(z, \delta z) = 1$ for completely coherent beams]. The influence of higher diffraction orders can be neglected because they carry low power and leave the interference region at characteristic values of mask displacement due to the large deviation angles.

The mean induced refractive index is

$$\overline{\Delta n}(z) = \delta m \Delta n_0 \left[\exp\left(-\frac{2(z-\delta z)^2}{w^2}\right) + \exp\left(-\frac{2(z+\delta z)^2}{w^2}\right)\right] + \delta m_0 \Delta n_0 \exp\left(-\frac{2z^2}{w^2}\right). \quad (2)$$

The minimum distance δl_0 between the phase mask and the optical fibre core is determined by the fibre diameter (125 μm) and is estimated to be ~100 μm (with allowance for

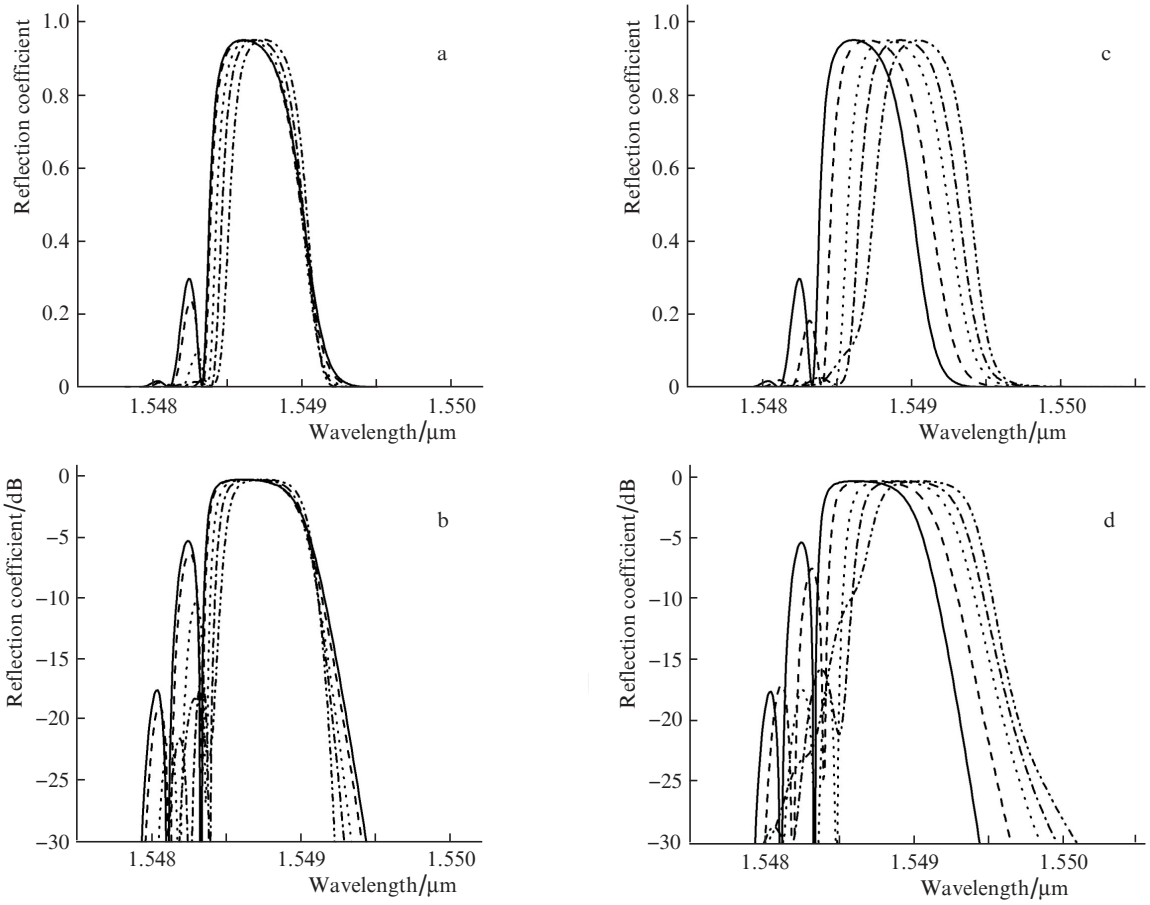

FBG spectra described by formula (1) at $f(z,\delta z) = 1$, with the parameters $w = 2$ mm; $\Lambda n_0 = 0.7741$ μm; and (solid line) $\delta z_0 = 0.01w$, $\Delta n_0 = 0.68 \times 10^{-3}$; (dashed line) $\delta z = 0.2w$, $\Delta n_0 = 0.72 \times 10^{-3}$; (dotted line) $\delta z = 0.4w$, $\Delta n_0 = 0.88 \times 10^{-3}$; (dash-and-dot line) $\delta z = 0.5w$, $\Delta n_0 = 1.04 \times 10^{-3}$; and (dash-and-double-dot line) $\delta z = 0.6w$, $\Delta n_0 = 1.26 \times 10^{-3}$ on (a) linear and (b) logarithmic scales and the FBG spectra described by formula (1) with allowance for (3) at $a = 2$ with the parameters $w = 2$ mm; $\Lambda n_0 = 0.7741$ μm; and (solid line) $\delta z_0 = 0.01w$, $\Delta n_0 = 0.68 \times 10^{-3}$; (dashed line) $\delta z = 0.2w$, $\Delta n_0 = 0.84 \times 10^{-3}$; (dotted line) $\delta z = 0.4w$, $\Delta n_0 = 1.17 \times 10^{-3}$; (dash-and-dot line) $\delta z = 0.5w$, $\Delta n_0 = 1.46 \times 10^{-3}$; and (dash-and-double-dot line) $\delta z = 0.6w$, $\Delta n_0 = 1.88 \times 10^{-3}$ on (a) linear and (b) logarithmic scales; Λn_0 is the optical length of the FBG line period.

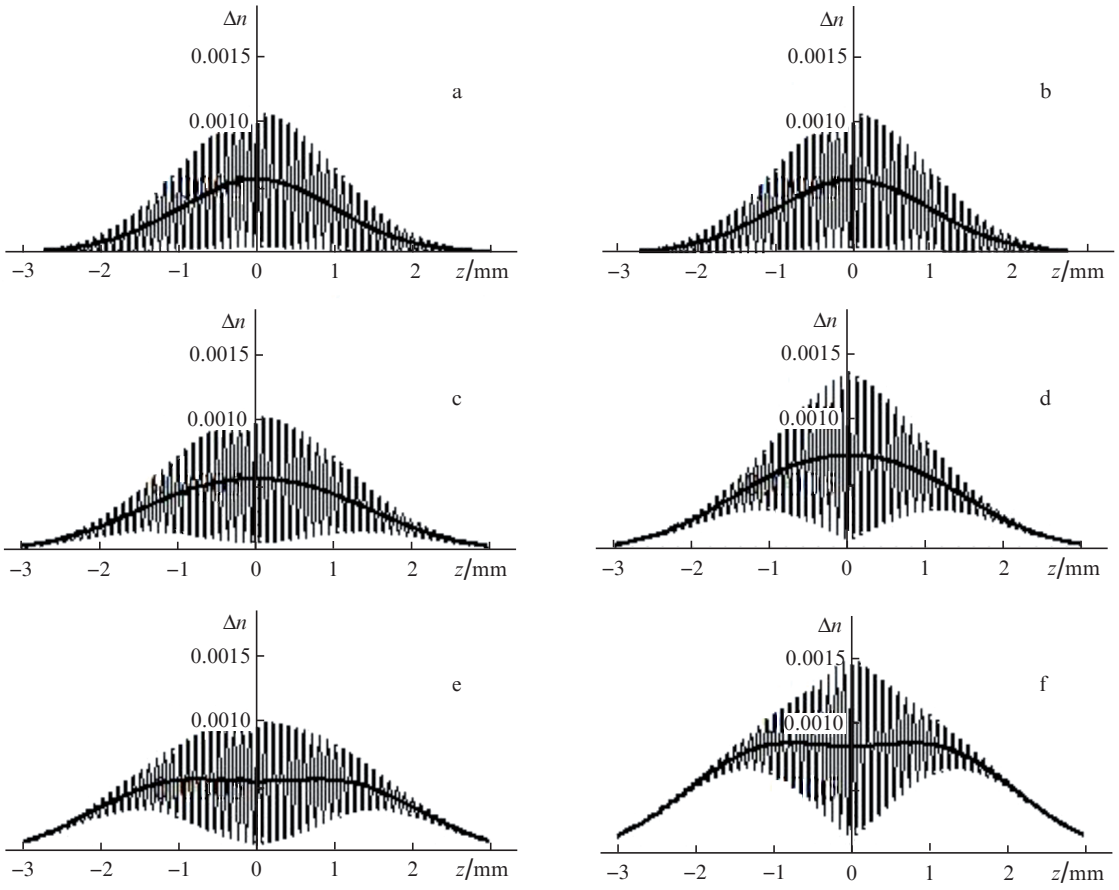

Figure 2. Refractive index profiles calculated from formula (1) at $f(z,\delta z) = 1$ for gratings with the parameter $w = 2$ mm at (a) $\delta z_0 = 0.01w$, $\Delta n_0 = 0.68 \times 10^{-3}$; (b) $\delta z = 0.4w$, $\Delta n_0 = 0.88 \times 10^{-3}$; and (c) $\delta z = 0.6w$, $\Delta n_0 = 1.26 \times 10^{-3}$ and the refractive index profiles calculated from formula (1) with allowance for (3) ($a = 2$) for gratings with the parameter $w = 2$ mm at (d) $\delta z_0 = 0.01w$, $\Delta n_0 = 0.68 \times 10^{-3}$; (e) $\delta z = 0.4w$, $\Delta n_0 = 1.17 \times 10^{-3}$; (f) $\delta z = 0.6w$, $\Delta n_0 = 1.88 \times 10^{-3}$. The bold line presents the mean induced refractive index calculated from formula (2). For clearness, the refractive-index modulation period Λ is increased to 100 μm.

gapping). Thus, in the absence of mutual displacement of the phase mask and fibre, the half distance δz_0 between the interfering beam axes is $\delta z_0 = \delta l_0 \tan\alpha \sim 20$ μm.

The left column in Fig. 2 presents the FBG reflection spectra, described by formula (1), for completely coherent beams [$f(z,\delta z) = 1$] at different values of the parameter δz with a reconstructed amplitude of the reflection coefficient $R = 0.95$ (the parameter Δn_0 was increased to this end) on the (a) linear and (b) logarithmic scales. It can be seen that an increase in the parameter δz reduces the amplitude of side lobes on the left approximately from –5 dB at $\delta z = 0.01w$ to –20 dB at $\delta z = 0.6w$, with a simultaneous decrease in the fundamental-resonance width (by approximately 20%). This behaviour of the spectra can be explained by the corresponding change in the mean refractive index. The left column in Fig. 3 contains profiles of induced refractive index calculated from formula (1) at $f(z,\delta z) = 1$ for the displacements δz = (a) $0.01w$, (b) $0.4w$, and (c) $0.6w$. The solid line corresponds to the mean value calculated from formula (2).

A known effect [1] is observed at $\delta z = 0.01w \approx 0$: the left and right parts of the grating with equal mean refractive indices form an interferometer, which yields short-wavelength resonances. An increase in δz due to the transverse mask displacement reduces variations in the mean refractive index at the length of interference pattern; this effect can qualitatively explain the decrease in the lateral-resonance amplitude in the short-wavelength region of the spectrum. Simultaneously, the effective grating length increases, which leads to main-peak narrowing.

Thus, the calculation shows that the use of transverse displacement of the phase mask with respect to the fibre in the method proposed, in contrast to [7], allows one to use a Gaussian beam in order to record (in a single stage) gratings with a large reflection coefficient and suppressed (to –20 dB) side lobes.

3. Experimental

The effect of suppression of side lobes while recording an FBG was experimentally verified on a phase-mask system for recording FBGs (Fig. 1). The source of 244-nm radiation was a cw argon laser with intracavity frequency doubling in a nonlinear BBO crystal [9].

UV-laser radiation passes through a cylindrical lens with a focal distance of 77.17 mm and a phase mask to arrive at an optical fibre, which is located in the focal plane of the lens. An FBG with a Bragg wavelength of ~1.55 μm is recorded in the interference region of the waves diffracted into the +1st and –1st orders of the phase mask. The profile of phase-mask lines ensures suppression of the power of zero diffraction order to ~7% and concentration of 75% power in the +1st and –1st orders; this power redistribution was taken into account in

the calculations. The phase mask was mounted on a mobile table, which made it possible to change the distance δl between the mask and optical fibre, as well as the distance $2\delta z$ between the axes of interfering beams ($\delta z = \delta l \tan\alpha$, $\alpha = 13.5°$). To determine the radius of a beam, its profile (along the fibre) was measured by a Newport power meter with a 10-μm aperture. The Gaussian beam radius w in the lens focus (recording region) was ~1.1 and ~1.8 mm in the experiments on recording gratings with reflection coefficients $R = 80$ and 95%, respectively.

FBGs were recorded in a Corning SMF-28e+ fibre, kept previously in a hydrogen medium at a pressure of 8 MPa for seven days. The laser power was ~50 mW and the time for recording an FBG with a reflection coefficient of 95% was 5–10 min, depending on the distance between the centres of interfering beams (the recording time increased with an increase in the distance between the phase mask and fibre).

The dependence of the induced refractive index on the UV irradiation dose is known to be nonlinear in the general case [10]. The dependence of the induced refractive index on the exposure time at a specified intensity was investigated in [7]. It was shown that, under our experimental conditions, an increase in the irradiation dose results in the following: first the induced refractive index increases to $\sim 10^{-3}$ linearly in the first approximation (with an error smaller than 10%), after which the linear dependence is transformed into a power law with a power of ~0.5.

Two series of FBGs with reflection coefficients of 80% and 95% were recorded in the experiment at different δz values (Figs 4, 5).

Figure 4 shows the spectra of relatively weak gratings ($R = 80\%$, $w \sim 1.1$ mm), which were recorded at a shorter exposure and, correspondingly, had a lower induced refractive index. The side lobes in the short-wavelength part of the spectrum were suppressed from –13 to –20 dB (without significant narrowing of the main reflection peak), even at a small displacement of the beam axes ($\delta z \sim 0.07w$).

Smoothing out the spectrum of 'dense' gratings ($R \geqslant 95\%$) is much more important for practice. In this case, the amplitude of short-wavelength side lobes for recording by a Gaussian beam using the standard phase-mask method reaches –5 dB (see the calculation results in Figs. 2a and 2b).

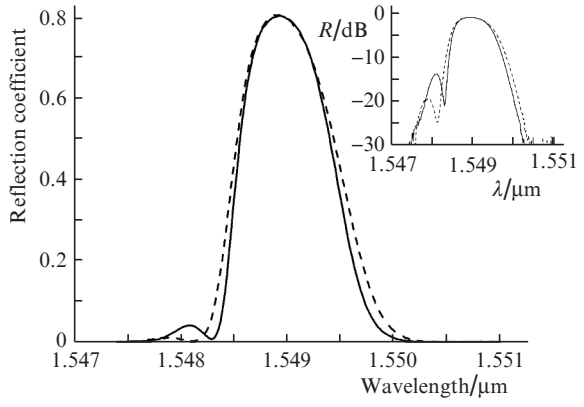

Figure 3. Experimental FBG spectra, recorded by a beam with a radius $w = 1.1$ mm, with the displacement parameters (solid line) $\delta z = \delta z_0 \approx 0.02$ mm and (dashed line) $\delta z = 0.074$ mm. The inset shows the reflection coefficient on the logarithmic scale.

The experimental reflection spectra of these FBGs ($R \sim 95\%$, $w \sim 1.8$ mm) are shown in Fig. 5. Indeed, when the optical fibre is closely fitting the phase mask ($\delta z = \delta z_0 \sim 0.01w$), the calculated amplitude of the side lobe is about –5 dB. When the parameter δz increases to $\sim 0.07w$, the lateral-resonance amplitude first decreases (as in the grating with $R = 80\%$) and then begins to grow; however, the lateral-resonance contrast decreases and, therefore, the spectrum is smoothed out. Although the experiment and theory show qualitatively similar behaviour of the grating having $R = 95\%$ with an increase in the δz, the shapes of the experimental (Fig. 5) and calculated (Figs 2a, 2b) reflection spectra, as well as the values of the optimal parameter δz, exhibit a significant discrepancy.

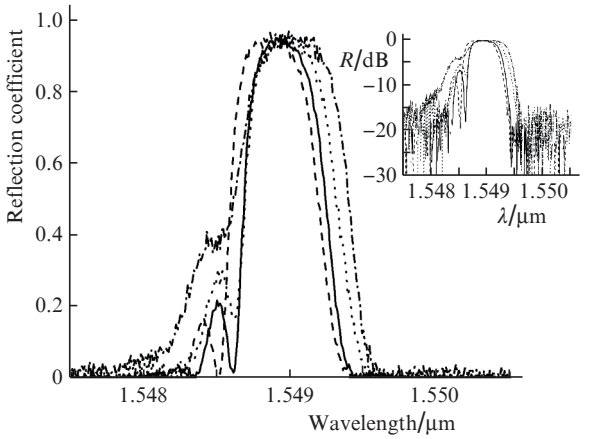

Figure 4. Experimental FBG spectra, recorded by a beam with a radius $w \sim 1.8$ mm, with the displacement parameters (solid line) $\delta z = \delta z_0 \approx 0.02$ mm, (dashed line) 0.074 mm, (dotted line) 0.26 mm, and (dash-and-dot line) 0.31 mm. The inset shows the reflection coefficient on the logarithmic scale.

In the experiment the lateral-resonance amplitude decreases more weakly than in the theory; nevertheless, the resonance structure is blurred with an increase in δz. Thus, the spectrum becomes relatively smooth (to a level of about –20 dB, which is determined by the measurement-scheme noise) even at $\delta z \approx 0.2w$. Here, in contrast to the calculated curves in Figs 2a and 2b, the main peak in the experimental reflection spectrum does not narrow but broadens and undergoes a red shift. A possible cause of this discrepancy between the experimental and theoretical data is that the calculation was performed disregarding the following factors: the decrease in the degree of coherence (and, correspondingly, blurring of the interference pattern at the periphery) with an increase in the relative displacement of the axes of interfering beams, the nonlinear dependence of the induced refractive index on the UV irradiation dose [7] (in simulation for large δz values the maximum amplitude $\Delta n(z = 0)$ reaches 10^{-3}; see Fig. 3c), laser beam divergence, and possible influence of vibrations of the measurement system base.

To take into account the decrease in the degree of coherence (and, correspondingly, the interference-pattern contrast) at a point z in the case of interference of oblique beams diffracted into the +1st and –1st orders, with centres shifted by δz, the following factor was introduced before the interference term into the formula for the induced refractive index:

$$f(z,\delta z) = \exp\left(-\frac{a\,|\,z\,|\,\delta z}{w_0^2}\right). \quad (3)$$

Figures 2c and 2d show the FBG reflection spectra described by formula (1) with the function $f(z,\delta z)$ given by (3) at $a = 2$ (note that the relationship between the effect under study and the parameters of the system should be additionally investigated), different δz values, and reconstructed amplitude of the reflection coefficient $R = 0.95$. It is found that the result of calculation using formula (1) taking into account the decrease in the degree of coherence at the periphery in correspondence with (3) ($a = 2$) is in much better agreement with the experimental data than the similar calculation with $f(z,\delta z) = 1$. This approximation describes qualitatively the main features of the experimental spectra: the red shift of the reflection spectrum without a significant change in the main-maximum width and the blurring of side lobes with an increase in δz, whereas in the case of completely coherent beams (Figs 2a, 2b) the spectral shift is much smaller than in the experiment and the side lobes do not change their shape (they are not blurred but decrease in amplitude).

The right column in Fig. 3 contains the profiles of induced refractive index calculated using formula (1) with regard to (3) for shifts $\delta z =$ (d) $0.01w$, (e) $0.4w$, and (f) $0.6w$. These profiles confirm that the decrease in coherence of interfering beams at the periphery leads to a sharper decrease in amplitude of the interference structure and the corresponding blurring of side lobes. The interference pattern becomes comparable in size with the region of constant mean, but the mean increases in comparison with the case of completely coherent beams (Fig. 3a), which leads to a shift of the spectral maximum, while the peak value of amplitude Δn exceeds significantly the limit (10^{-3}) of the linear dependence of the amplitude of the induced refractive index on exposure. This means that, when comparing the experimental results with theoretical predictions, one must take into account the dose dependence nonlinearity. This and some other ignored effects (beam divergence, the corresponding deviations of the wave front from planar, and vibrations) can explain the quantitative difference between the theoretical and experimental data.

4. Conclusions

Our calculation showed that the phase-mask scheme can be used to suppress significantly (to –20 dB) the side lobes of dense ($R = 95\%$) FBGs (without broadening the reflection spectrum) using a relative shift of the centres of interfering Gaussian beams with a radius w by $\delta z \sim 0.6w$ due to the transverse displacement of the phase mask. The predicted suppression is experimentally observed; however, the experimental value of the optimal displacement ($\delta z \sim 0.2w$) is much smaller. An additional calculation showed that this difference can be due to the decrease in the degree of coherence of interfering beams at the periphery with an increase in the distance δz between their centres. In addition, consideration of this effect allows one to describe theoretically (at the qualitative level) the experimentally observed 'blurring' of lateral peaks and red shift of the main peak in the reflection spectrum with an increase in δz. The quantitative discrepancies between the theory and experiment can also be caused by the nonlinear dependence of the induced refractive index on the irradiation dose at large displacements, laser beam divergence, and vibrations of the system base.

In the case of looser ($R = 80\%$) gratings, recorded at shorter exposure times, suppression of side lobes to a level of –20 dB in the experiment is observed at smaller displacements ($\delta z \sim 0.1w$), without any significant 'blurring' and changing the spectral shape.

Thus, it was shown that the phase-mask scheme for recording FBGs with transverse displacement of the phase mask with respect to the fibre, makes it possible to record gratings with a fixed Bragg wavelength and smoothed side lobes without a significant change in the spectral width. The side lobes in the short-wavelength region are smoothed out due to the relative shift of the centres of interfering beams and equalisation of the mean refractive index in the region of FBG recorded. This simple apodisation technique is promising for many FBG applications in fibre optics, in particular, mirrors of fibre laser cavities and precise fibre sensors with spectral multiplexing, which need a smooth spectral profile. This apodisation technique imposes no limitations on FBG application. The use of the above-described method in the scheme based on a phase mask and a two-mirror interferometer will make it possible to record FBGs with suppressed side lobes at an arbitrary wavelength in the spectral range 1–1.6 μm.

Acknowledgements. We are grateful to A.A. Vlasov for his help. This work was supported by grants of the Ministry of Education and Science of the Russian Federation and an integration project of the Siberian Branch of the Russian Academy of Sciences.

References

1. Kashyap R. *Fiber Bragg Gratings* (San Diego: Acad. Press, 1999).
2. Vasil'ev S.A., Medvedkov O.I., Korolev I.G., Bozhkov A.S., Kurkov A.S., Dianov E.M. *Kvantovaya Elektron.*, **35**, 1085 (2005) [*Quantum Electron.*, **35**, 1085 (2005)].
3. Erdogan T. *J. Lightwave Technol.*, **15**, 1277 (1997).
4. Othonos A., Kalli K. *Fiber Bragg Gratings: Fundamentals and Aplications in Telecommunications and Sensing* (Norwood: Artech Hous, 1999).
5. Loh W.H. et al. *Opt. Lett.*, **20**, 2051 (1995).
6. Tikhomirov A., Foster S. *J. Lightwave Technol.*, **25**, 533 (2007).
7. Abdullina S.R., Babin S.A., Vlasov A.A., Kablukov S.I. *Kvantovaya Elektron.*, **36**, 966 (2006) [*Quantum Electron.*, **36**, 966 (2006)].
8. Belai O.V., Podivilov E.V., Shapiro D.A. *Opt. Commun.*, **266**, 512 (2006).
9. Abdullina S.R., Babin S.A., Vlasov A.A., Kablukov S.I. *Kvantovaya Elektron.*, **35**, 857 (2005) [*Quantum Electron.*, **35**, 857 (2005)].
10. Medvedkov O.I., Korolev I.G., Vasil'ev S.A. Preprint NTsVO No. 6 (Moscow, 2004).